Received 20 December 2021; revised 14 February 2022; accepted 22 February 2022. Date of publication 25 February 2022; date of current version 16 June 2022.
The review of this article was arranged by Editor B. Iñiguez.

Digital Object Identifier 10.1109/JEDS.2022.3154538

Using Self-Heating Resistors as a Case Study for Memristor Compact Modeling

RODRIGO PICOS [1] (Senior Member, IEEE), MOHAMAD MONER AL CHAWA [2] (Member, IEEE), CAROLA DE BENITO [1] (Senior Member, IEEE), STAVROS G. STAVRINIDES [3] (Senior Member, IEEE), AND LEON O. CHUA [4] (Life Fellow, IEEE)

1 Industrial Engineering and Construction Department, Universitat de les Illes Balears, 07122 Palma, Spain
2 Faculty of ECE, Technical University Dresden, 01069 Dresden, Germany
3 School of Science and Technology, International Hellenic University, 57001 Thermi, Greece
4 EECE Department, University of California at Berkeley, Berkeley, CA 94720, USA

CORRESPONDING AUTHOR: R. PICOS (e-mail: rodrigo.picos@uib.es)

This work was supported by the Spanish Ministry of Science under Project DPI2017-86610-P and Project TEC2017-84877-R (also supported by the FEDER Program).

ABSTRACT Memristors were first proposed in 1971 by Leon Chua. These devices are usually regarded as being one of the newest fundamental breakthrough for electronics. Their role in designing new electronic systems is expected to be an important, key-factor. As an example, they already come in many forms: PCA, ReRAM, etc., to mention a few. In any case, since actual memristors have only appeared quite recently, this technology has yet to be mature enough to provide with readily available, off-the-shelf components. This implies that developing and testing new concepts or design architectures based on memristors are performed mainly by the use of numerical simulation. In this paper, we discuss a powerful modeling framework that eases creating and implementing new memristor models, illustrating with some examples of use.

INDEX TERMS Memristor, RRAM, compact modeling, thermistor.

I. INTRODUCTION

It has been proposed that there is an apparent symmetry pattern in the relations between the four fundamental electrical magnitudes (current i, voltage v, charge q and flux φ). This passed unnoticed for many years in circuit theory until Chua, at the early 70s, proposed the axiomatic definition of a fourth electrical element, which was named the Memristor [1]. Its name originated from the fact that such an element unified in one element resistor and memory, having these two properties combined. Besides, Chua's work led to the generalization of a class of devices as well as systems that are inherently nonlinear and governed by a state-dependent, algebraic relation accompanied by a set of differential equations, which are called memristive systems or devices [2]. As an interesting fact, it has to be said that memristors had actually been described many years ago [3], but they had never made it to the mainstream of electrical or circuit theory since the non-linear theory needed was not developed till recently.

The inherent memory feature embodied in memristors has led these novel devices to be considered as one of the key technology enablers of a technological breakthrough in integrated circuit (IC) performance growth, beyond and more than Moore [4]. Among others, they are expected to allow for easy in-memory computation, thus providing with a solution to the classical bottleneck problem in data transmission between memories and processors. Other areas that are expected to benefit from the use of memristors and memristive systems are the IoT and other edge computing applications, where they can be changing radically the related technological landscape. Thus, an increasing number of memristor-based applications has already been proposed; indicatively, new kind of memories (ReRAMs, MRAM, etc.) [5]–[7], innovative new sensor devices [8], [9], or basic building elements for bio-inspired systems (ANNs) [10].

These devices can be built in a wide range of technologies, from spintronics [11] to organic materials [12], [13]

and many different oxides [14]–[17]. Unfortunately, few foundries are including memristors as a standard element in their libraries, as it customarily happens with resistors or capacitors. In fact, and up to the best of our knowledge, RRAMs can be obtained at TSMC, Towerjazz and Intel, and only for old nodes. This, which may seem to be a drawback, can be considered an advantage to implement low-cost edge platforms [18].

Simulating a new design incorporating memristors (usually RRAMs) is not something straightforward; many good models have been proposed, both using the classical approach that utilizes current and voltage [19]–[23], or the charge and flux approach [24]–[29], which had been historically used in oxide breakdown. However, most of these models appear to demonstrate drawbacks that make simulation of large circuits rather difficult or even impractical [30]. Besides, there are still some open problems in modeling memristor: the variability they exhibit from cycle to cycle [31]–[33], noise [34], [35], and, mainly, the development of predictive compact models. The later is, however, impaired by the fact that it seems to be some inherent randomness into the transitions from low to high resistance state and, in a minor way, from low to high.

In this paper we will study the case of self-heating resistors as a paradigmatic case of a device with memory. This study will be performed by formulating their governing equations inside the memristor formalism, as proposed by [36]. This will allow us to deal with these devices as memristors, as was already proposed by Chua and Kang in [2].

II. UNIFIED FORMALISM FOR MEMRISTOR MODELING

A most useful workspace for memristor modelling was introduced by Corinto *et al.* in [36] where the authors develop a unified theoretical framework and also discuss the advantages of using the flux–charge (φ-q) domain to study memristor elements. In this framework, the memristors in the taxonomy proposed in [37] (the ideal, the generic, and the extended memristor) are described as different approximations in the equations. This extended categorization emerged as a necessity in order to include theoretically the description of pinched, hysteretic behaviors demonstrated by various elements, not only in circuit theory and electronics but also in nature.

Among the different categories presented above, the most general class are extended memristors, which refers to memristors that have extra state variables $\mathbf{X} = (X_1, X_2, \ldots)$ (in addition to φ and q). The general relation describing them cen be written as:

$$\varphi = f(Q, i, \mathbf{X}) \tag{1}$$

where the flux (φ) and the charge (Q) are related to the voltage (v) and the current (i) respectively as:

$$\frac{d\varphi}{dt} = v \tag{2}$$

$$\frac{dQ}{dt} = i \tag{3}$$

In addition, there is also the description of the evolution of the internal variables $\mathbf{X}$, which is performed in terms of a differential equation:

$$\frac{d\mathbf{X}}{dt} = \mathbf{g_Q}(Q, i, \mathbf{X}) \tag{4}$$

The relation between voltage and current (i.e., the equivalent to Ohm's law) is obtained by deriving Eq. (1) with respect to time:

$$v = \frac{d\varphi}{dt} = \frac{\partial f(Q,i,\mathbf{X})}{\partial Q}\frac{dQ}{dt} + \frac{\partial f(Q,i,\mathbf{X})}{\partial i}\frac{di}{dt} + \sum_j \frac{\partial f(Q,i,\mathbf{X})}{\partial X_j}\frac{dX_j}{dt} = \frac{d\varphi}{dt} = \frac{\partial f(Q,i,\mathbf{X})}{\partial Q} i = \frac{\partial \varphi}{\partial Q} i \tag{5}$$

This result is obtained under the premise [36] that:

$$\frac{\partial f(Q,i,\mathbf{X})}{\partial i}\frac{di}{dt} + \sum_j \frac{\partial f(Q,i,\mathbf{X})}{\partial X_j}\frac{dX_j}{dt} = 0 \tag{6}$$

Notice that the above assumption has a physical meaning, since the terms in Eq. (6) can be identified with parasitic components. Specifically, the term with di/dt can be related to an inductive parasitic element, and the terms in dX_j/dt correspond to voltage sources.

Thus, we can define the memristance M to be:

$$M(Q, i, \mathbf{X}) = \frac{\partial \varphi}{\partial Q} = f_M(Q, i, \mathbf{X}) \tag{7}$$

Notice that should the description be done using flux and voltage as the variables, the parasitic components would have been capacitors and current sources [36].

As a summary, the final relations for a charge-controlled memristor are described by Eqs. (3), (4) and (8):

$$v = M(Q, i, \mathbf{X}) \cdot i \tag{8}$$

The memristance M of an extended memristor is implied in Eq. (8), apparently bearing the feature of nonlinearity; v is the voltage across the memristor, i is the current flowing through it, and Q the charge, i.e., currents's first momentum. The vector x stands for a set of extra state variables, including all the necessary physical magnitudes according to the implemented memristive system; indicatively they could be the internal temperature, the radius of a conducting filament, or any other non-electrical variable influencing the state of the memristor. Apparently, the dynamics of the state variables X are governed by g_Q and Eq. (4). It is noted that the importance of the class of extended memristors, comes from the fact all the known until now, real-world memristor devices, are indeed extended memristors.

A special case of Eq. (4) is often referred to as the power–off plot (POP) equation and determines the memory capability of the system under no excitation; in this case for $dQ/dt = i = 0$. It is clear that if the POP equation is nil under these conditions, the system presents a long–term memory since the state variable will not change with time, while if it is different than zero, the system is capable of exhibiting only short–term memory.

III. THE THERMISTOR

The thermistor is one of the oldest devices identified to possess the characteristics of a memristor [2], [38], [39]. The model has been known since John Steinhart and Stanley Hart published a function, modeling the variation of thermistor-resistance according to temperature [40]. This function, along with the equivalent Ohm's law in Eq. (9), shown in Eq. (10), has proved to be suitable in a wide variety of thermistors, for ranges from a few degrees to a few hundred degrees, and has been widely used to model this kind of devices when used as temperature sensors. In addition, a key characteristic of thermistors is that they undergo self-heating, which can be described by Eq. (11).

$$v = M(T)i \tag{9}$$

$$M(T) = R_0 e^{B\left(\frac{1}{T}-\frac{1}{T0}\right)} \tag{10}$$

$$\frac{dT}{dt} = Mi^2 - \frac{\delta}{C_{pm}}(T - Ta) \tag{11}$$

In the above equations, T_a is the ambient temperature, and T the internal temperature of the device. The rest of the symbols are parameters of the thermistor model, and can be considered as constants for practical purposes. At this point, it is impossible escape noticing that these equations bear exactly the same form with the equations defining the memristor ((8), (7) and (4), respectively). Thus, we can identify the thermistor as being a memristor. That is, the thermistor is a system whose resistance depends on its electrical history, and has an internal variable that governs the overall behavior (internal temperature). Thus, the system is classified as an extended memristor.

In addition, if we look at the POP equation (Eq. (11) with $i = 0$), we see that it is different from zero for any situation other than thermal equilibrium with the environment. Thus, the system does not possess the feature of long term memory. In these aspects, it is also illustrative to point out that there are other dissipative systems [41] that are also memristors due to self-heating, even if the specific mechanism is very different than that of thermistors.

To illustrate this memristive behavior, we have driven a thermistor by a triangular current waveform. We have used the following values for the thermistor constants: $\delta \approx 4 \cdot 10^{-3} W/K$, $C_{pm} \approx 60 \cdot 10^{-3} K^{-1} s$, $B = 3950K$, $T_0 = 298K$, $T_a = 300K$, $R_0 = 10k\Omega$. Additionally, and in accordance with a typical thermistor datasheet, we have set a maximum current of 4.5 mA, and we have also used 5 different ramp speeds. The results are shown in Fig. 1, where the evolution of the resistance (mem-resistance) and the current input versus time, are shown. The resistance versus the input current is shown in Fig. 2. From these figures, we can draw the typical plots of a memristor in the I-V plot, as depicted in the classical seagull wings in Fig. 3.

We can compare the results shown in those figures against the two fingerprints of a memristor [42]: a pinched loop, whose area changes with frequency, tending to a line at high frequency. Those effects are caused, in our system, by

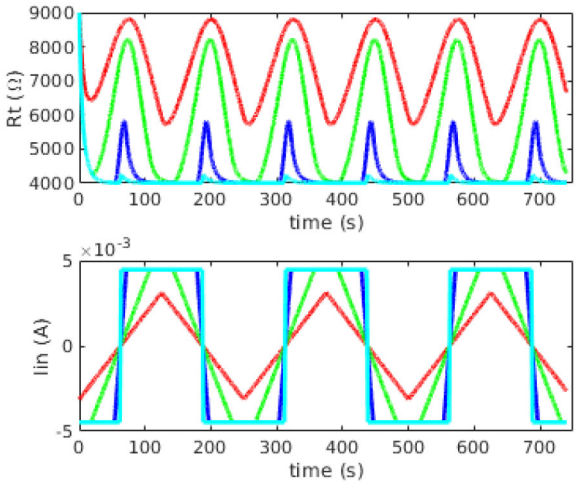

FIGURE 1. Evolution of input current waveform (bottom) and memristance (top) versus time, for four different slope velocities. Colors are coherent for both plots.

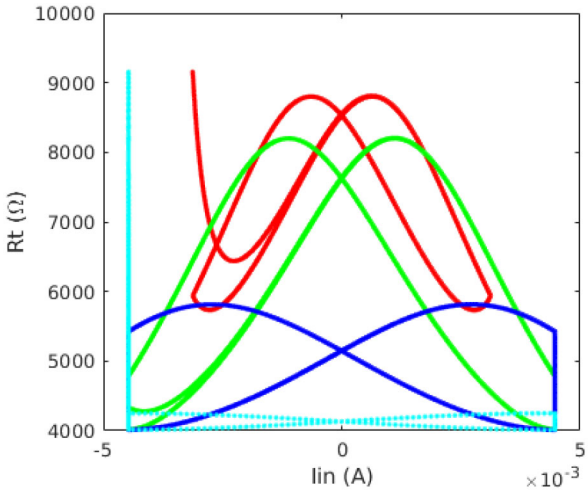

FIGURE 2. Evolution of memristance versus input current waveform, for four different slope velocities. Colors are coherent with Fig. 1.

the dissipative system described by Eq. (11). This equation means that, at low frequency (where the system may be considered to be in thermal equilibrium with the environment, so $dT/dt \approx 0$), the system tends to a nonlinear resistor, as shown in the Figures (dark blue and red lines). On the other hand, at high frequency, the thermal capacitance is so high that $dT/dt \approx Mi^2$, and we can see that the highest frequency ramp (cyan line) is, in fact nearly an ohmic resistor. It has to be noted that, in this case, likewise in [41], the situation is more complex than that of an ideal memristor, since the thermistor is a *dissipative* device, as seen in Eq. (11).

At this point, it is also convenient to introduce some notions from the theory of nonlinear dynamics, since it seems to be convenient in analyzing the system. The first concept to understand how the thermistor behaves is its *trajectories*, which are describing the evolution within the phase space of the system. In our case, the *free* variable is the input current,

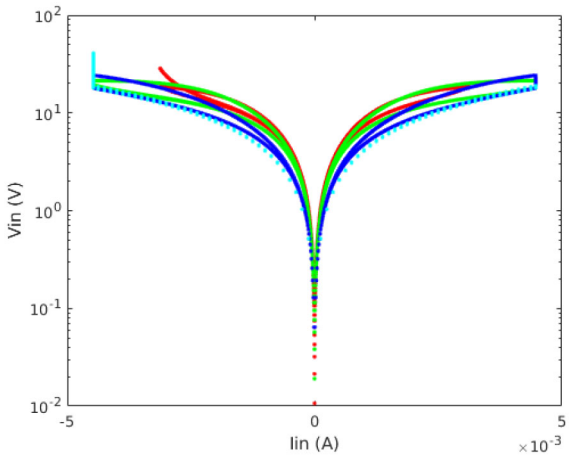

FIGURE 3. I-V characteristics of the thermistor for four slopes. Colors are coherent with Fig. 1.

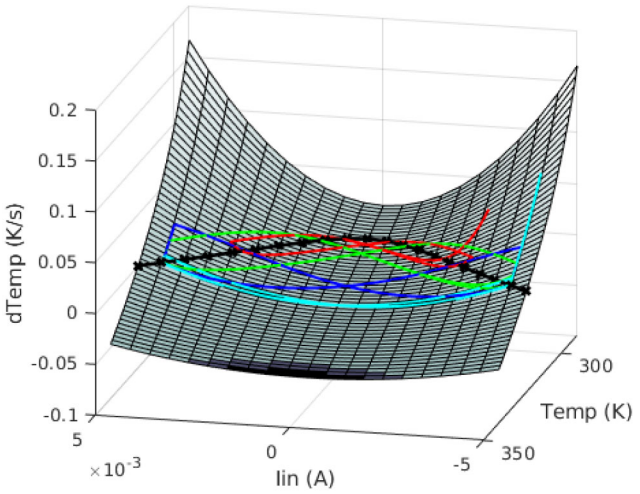

FIGURE 4. Dynamic Route Map of the memristor (surface), showing the four trajectories of the previous figures, using the same colors. The black, thick line represents the points where dT/dt = 0.

and the system is well-determined by two more variables. These could be the temperature and the device's memristance (Eq. (10)), or the temperature and the derivative of the temperature. Actually, the best option is the last one, since it represents the behavior of the internal state variable. This leads us to the second important concept: the *Dynamic Route Map* (DRM) [43], [44].

The DRM is a representation of the trajectories that the system can follow in the phase space of the state variable versus its derivative, for different values of a control parameter. This map provides with very useful information about the behavior of the system. For instance, if a trajectory goes from positive derivative to negative derivative values with increasing temperature, then the temperature at which it nullifies is what is called a *stable equilibrium point*. An equilibrium point is a state where the system tends to go and remain at, similar in concept to what is called the quiescent point in circuit theory. On the other hand, if the trajectory goes from negative to positive, the crossing point is also an equilibrium point, but *unstable*, which means that the slightest change will force the system out of it. In addition, if we plot it as a 3D diagram, we see that all the trajectories, for constant T_a, must fall over the same surface, as can be seen in Fig. 4.

As an application example of the above notion, a faster method for reading temperature is proposed, and it is considered as a future work. This application is based on the fact that thermistor-operation is usually set in the curves over this DRM surface, where $dTemp/dt = 0$; since this means that the system has reached thermal equilibrium. Also worth of interest is the fact that this DRM surface is parameterized by T_a. Thus, one can envision a readout system that takes profit from this memristive description and uses the dynamic behavior of the thermistor to identify this surface and, consequently, the ambient temperature in a faster way than conventional systems.

IV. USING THE DRM FOR EMPIRICAL MODELING

As has been seen in the previous section, the DRM can be a very useful tool for interpreting the behavior of a memristor. In this section, we propose using this DRM to perform empirical modelling of a specific device, given its electrical i-v curves. Specifically, we will be using data coming from a light bulb back from the time when these devices used self-heating to emit light [41], [45].

A. EXPERIMENTAL SETUP

In order to explore experimentally the electrical behavior of filament bulbs, a 6V incandescent flashlight bulb, operating within its voltage/power limits, was utilized. This bulb contained a tungsten filament, electrically heated at about 2400 K (tungsten melting point is 3695 K) in a vacuum ambient (under 2800 K no inert gas is needed to withstand evaporation of the tungsten filament atoms).

The measurement methodology was very simple and included current-driven $i - v$ measurements, by applying a sinusoidal current of $i_{p-p} = 200$mA, for a variety of frequencies (f), ranging from 0.01Hz to 10Hz. A custom-made automated measurement setup included a Pico Technology ADC-24 data-logger, which allowed for the monitoring of both current and voltage. All sampling rates were continuously adjusted in such a way that the same number of data points (typically 8000 points) were acquired for each frequency of the applied sinusoidal current. It is noted that all measurements were recorded, after dynamic equilibrium had been reached.

In Figure 5 the experimental $i-v$ characteristic appears for four typical individual cases of sinusoidal and also triangular current-excitation frequencies, namely at 0.01Hz, 0.1Hz, 1Hz and 10Hz, driving the same incandescent bulb. From these figures, is apparent that a non-ohmic, memristive behavior is demonstrated at these frequencies (less than 10Hz), being present from the very low frequencies (10mHz), while it is gradually replaced by linear $i-v$ curves (from 10Hz and on), clearly hinting to the ohmic behavior expected for memristors when $f \to \infty$ [36]. This means that the memristive behavior

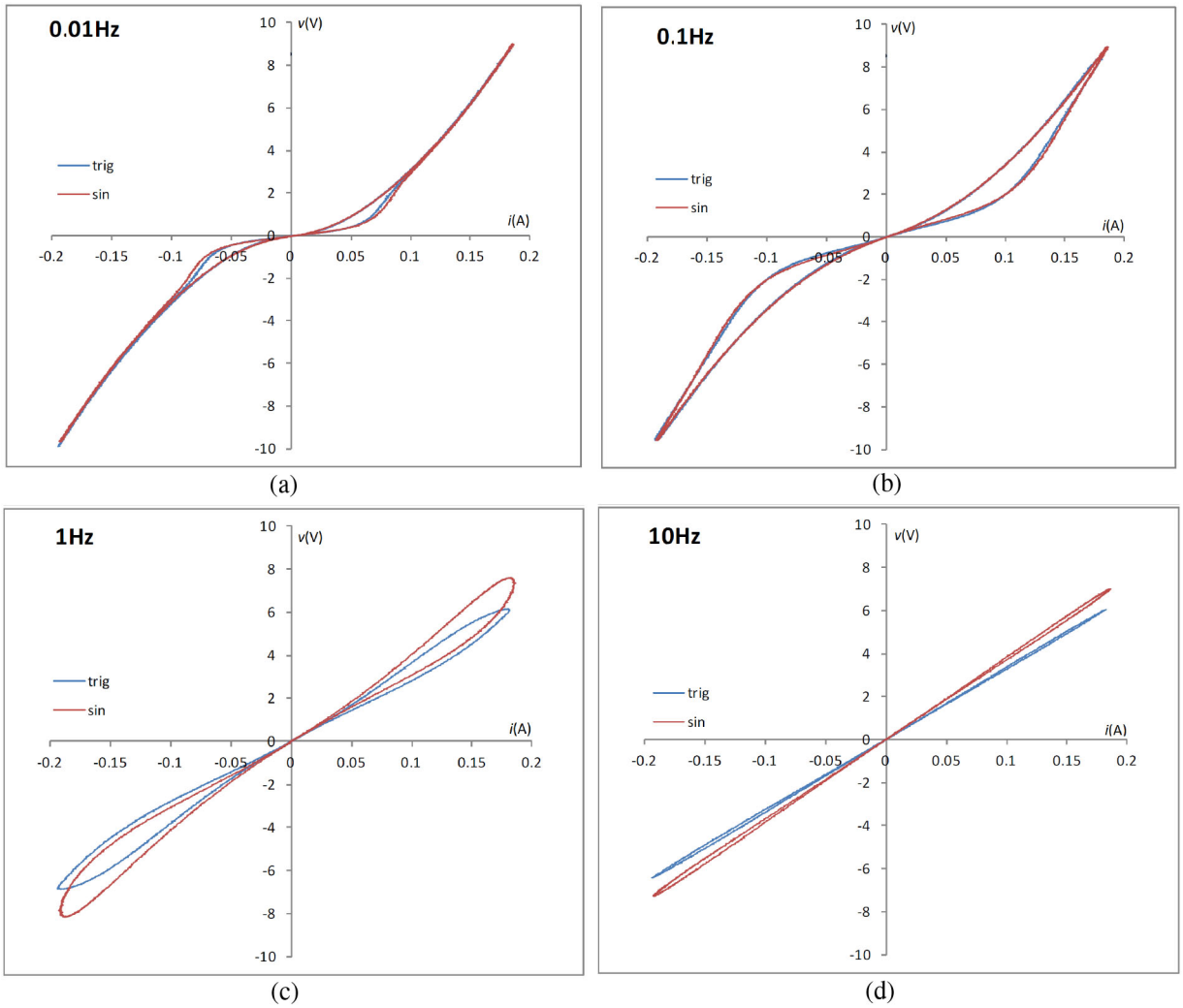

FIGURE 5. **Experimental $i - v$ characteristic curves of a tungsten filament bulb driven by a sinusoidal (red lines) and a triangular (blue lines) current, for 4 different representative frequencies (a) 0.01 Hz, (b) 0.1 Hz, (c) 1 Hz, and (d) 10 Hz. It is obvious that in the last case the heated filament demonstrates a near-ohmic behavior, as expected for generic and extended memristors when $\omega \to \infty$.**

of incandescent bulbs is deployed for driving frequencies less than 10Hz. From that frequency and on the filament's resistivity is becoming constant, as predicted in the case of memristive devices [36].

The distortion of the voltage signal, typical of memristive systems, is apparent due to a hysteresis in the response, which is the result of the thermal dynamics of the system comprised by the filament and the bulb shell. In specific, this is mainly due to the heat capacity and the heat diffusion mechanisms of the filament [45], [46].

B. PHYSICALLY-BASED MODEL

The tungsten filament bulb's hysteretic behavior has been already reported in [46] and a mathematical model describing the physical mechanisms behind this behavior has been introduced. The proposed model was very accurate and slightly more complex than the copper wire memristor model presented in [47]. The idea behind the derivation of those models is to consider the power balance between the power provided by the external source $V(t)$, the power stored because of self-heating, and the radiated power; this leads to the following equation, as derived in [46]:

$$\frac{V^2(t)}{\rho(T)} = c(T)L^2\frac{dT}{dt} + e\sigma\sqrt{\frac{4\pi R_0 L^3}{\rho_0}}\left(T^4 - T_0^4\right) \qquad (12)$$

where $\rho(T)$, $c(T)$ and L are resistivity, the volumetric heat capacity and the length of the tungsten filament, respectively, e is the emissivity of the filament and σ is the Stefan-Boltzmann constant. All magnitudes bearing a zero (0) indicator refer to the corresponding magnitude at the ambient temperature. In this model and for the temperature range of low voltage flashlight bulbs, absorption of radiation, as well as, convection and conduction were supposed to be negligible; something that was also verified in [17]. From equation (12), one could calculate the filament's temperature $T(t)$, leading then to the calculation of $R(t)$ and finally the calculation of $i(t)$.

Taking advantage of the proposed model described by [46, eq. (12)] and in order to accentuate the memristive features of the presented experimental behavior of incandescent bulbs, a modified model based on the typical formulation proposed in [36], [48], is presented hereby. In this model, the filament is of length L, with a uniform area A, and its temperature $T(t)$ is considered as the state variable and in the case of a flux-controlled memristor (voltage-driven), it is described by the following set of equations:

$$i(t) = W(T, q, i, t) \cdot v(t) \tag{13}$$

$$W(T, q, i, t) = \frac{A}{L \cdot \rho(T)} \tag{14}$$

$$\frac{dT}{dt} = \frac{v^2(t)}{L^2 c(T)\rho(T)} - \frac{e\sigma\sqrt{4\pi R_0/\rho_0}}{c(T)\sqrt{L}} \cdot \left(T^4 - T_0^4\right) \tag{15}$$

$$\rho = \rho_0 \cdot \left(1 + \rho_1 T + \rho_2 T^2\right) \tag{16}$$

$$c(T) = c_0 + c_1 T + c_2 T^2 + + c_3 T^3 + \frac{c_4}{T^2} \tag{17}$$

where $W(T, q, i, t)$ is the device's *memductance*. In equation (16) resistivity is described according to [49], while the volumetric heat capacity $c(T)$, described in equation (17), is given by the Shomate equation [50]. The values of the coefficients in both equations are listed in the corresponding references.

C. EMPIRICAL MODELING

In the above subsection we have described the physically-based model for the system. It has to be noted that this includes many approximations, such as that $c(T)$ and $\rho(t)$ are approximated as power series, or that the effect of the bulb crystal shell is ignored, etc. All these approximations are performed in order to obtain an explicit form for Eq. (15).

Here, we propose that these approximations were replaced by a direct approximation for the variation of the memristance:

$$i = Mv \tag{18}$$

$$\frac{dM}{dt} = g_M(M, v) \tag{19}$$

Once we consider this description, it is worth noticing that Eq. (19) corresponds to a DRM. It is apparent that now one can calculate an approximation to dM/dt from the experimental data, and plot it against M and i. We have performed this kind of calculation and the results are illustrated in Fig. 6. Once this is performed, we have fitted a polynomial approximation (MATLAB *polyfit53*) to these curves, which is in fact an approximation to g_M.

$$g_M(M, v) \approx \sum_{i=0..5, j=0..3} p_{i,j} v^i M^j \tag{20}$$

The coefficients $p_{i,j}$ are provided in Table 1, along with the 95% confidence interval, as provided by MATLAB.

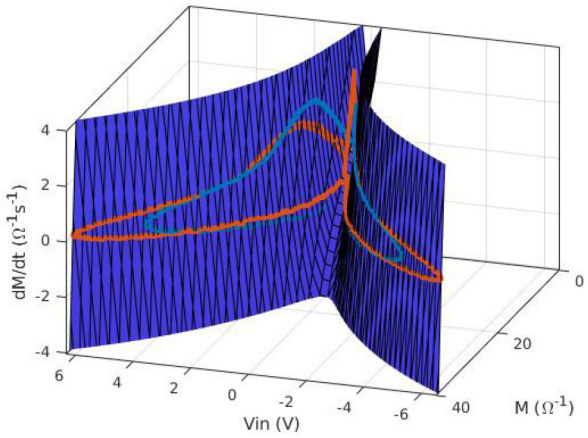

FIGURE 6. DRM for the experimental data (color lines), and fitted surface equivalent to Eq. (19) (surface).

TABLE 1. Coefficients for the approximation of g_M in Eq. (20). The units for coeffient p_{ij} are $s^{-1}V^{-i}\Omega^{j-1}$.

Coefficient	Value	95% Confidence
p_{00}	1.874	(1.189, 2.558)
p_{10}	0.07793	(-1.17, 1.326)
p_{01}	-0.4581	(-0.6641, -0.2522)
p_{20}	17.49	(15.72, 19.26)
p_{11}	-0.0519	(-0.2794, 0.1756)
p_{02}	0.02412	(0.005537, 0.0427)
p_{30}	-0.2097	(-0.5823, 0.1628)
p_{21}	-1.338	(-1.548, -1.127)
p_{12}	0.003535	(-0.01004, 0.01711)
p_{03}	-0.001308	(-0.00184, -0.0007755)
p_{40}	-0.1169	(-0.1628, -0.07104)
p_{31}	0.01048	(-0.01018, 0.03114)
p_{22}	0.04049	(0.03192, 0.04906)
p_{13}	-0.00005741	(-0.0003187, 0.0002039)
p_{50}	0.0002386	(-0.001799, 0.002276)
p_{41}	0.002796	(0.00168, 0.003913)
p_{32}	-0.0001394	(-0.0004952, 0.0002165)
p_{23}	-0.0004267	(-0.0005411, -0.0003124)

In order to check the validity of this method, we have used the described above polynomial approximation to predict the evolution of another signal at 0.05 Hz. To do so, we have used Equation (18) and (19), where g_M is the fitted approximation. Integration of these equations provides the results in Fig. 7, where the magenta lines are the model and the blue lines correspond to experimental data. The initial condition for M has been considered as the experimental M at the initial instant. Notice that the noise is caused by the numerical calculation of dM/dt. The coincidence between the real data and the predicted by the model values is evident.

V. CONCLUSION

Memristor is postulated as the most recent significant breakthrough in electronics. However, since actual memristors have appeared quite recently, memristive technologies are not mature enough to allow for providing with readily available, off-the-shelf memristors or memristive components in general. This implies that developing and testing new concepts or design architectures based on memristors are performed mainly by the use of numerical simulation.

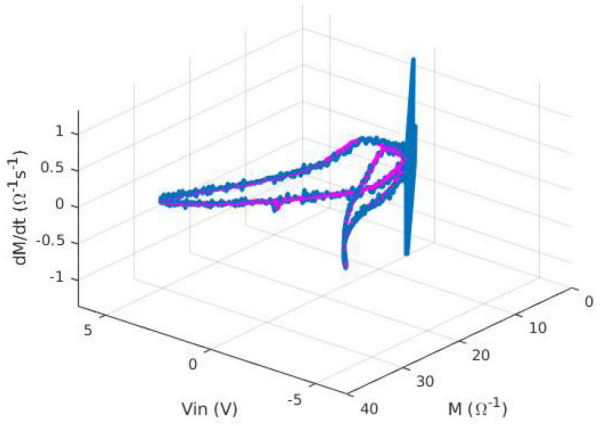

FIGURE 7. Experimental (blue line) and calculated response of the system using the approximation given by Eq. (20) and the coefficients in Table 1 (magenta line).

Taking all the above into account, in this paper we present a formal framework for memristor compact modeling. Based on this we have then shown that a thermistor, a well-known nonlinear device, can be given a twist and used as what it really is, i.e., as a memristor. This way, it served as an example of using the introduced modeling framework. Within this framework, next to the standard analysis procedure that includes the investigation of demonstration the essential fingerprints of a memristor (the pinched hysteresis loop, whose enclosed area tends to zero at high frequency), a rather novel tool, the Dynamic Route Map (DRM), has also been utilized.

In order to exemplify the utilization of the DRM as a modeling tool, wIn order to exemplify the utilization of the DRM as a modeling tool, we have also used it to model a self-heating memristive device. Applying the idea, we have experimentally obtained the DRM, using as variables of interest the device's memristance, its temporal derivative, and the applied voltage. Fitting a polynomial to this experimental surface allowed for a very precise prediction of the beha

We have also used it to model a self-heating memristive device. Applying the idea, we have experimentally obtained the DRM, using as variables of interest the device's memristance, its temporal derivative, and the applied voltage. Fitting a polynomial to this experimental surface allowed for a very precise prediction of the behavior of the device under consideration at a different frequency.

Finally, possible applications of the proposed compact modeling method are considered as future work, like the possibility of designing a temperature readout system that takes profit from this memristive description, using thermistor's dynamic behavior of to identify the ambient temperature in a faster way than conventional systems.

REFERENCES

[1] L. O. Chua, "Memristor-the missing circuit element," *IEEE Trans. Circuit Theory*, vol. 18, no. 5, pp. 507–519, Sep. 1971.
[2] L. O. Chua and S. M. Kang, "Memristive devices and systems," *Proc. IEEE*, vol. 64, no. 2, pp. 209–223, Feb. 1976.
[3] T. Prodromakis, C. Toumazou, and L. Chua, "Two centuries of memristors," *Nat. Mater.*, vol. 11, no. 6, pp. 478–481, 2012.
[4] R. Tetzlaff, *Memristors and Memristive Systems*. Cham, Switzerland: Springer, 2013.
[5] H. Kim, M. P. Sah, C. Yang, and L. O. Chua, "Memristor-based multilevel memory," in *Proc. 12th Int. Workshop Cellular Nanoscale Netw. Their Appl. (CNNA)*, 2010, pp. 1–6.
[6] S. Stathopoulos *et al.*, "Multibit memory operation of metal-oxide bi-layer memristors," *Sci. Rep.*, vol. 7, no. 1, pp. 1–7, 2017.
[7] K. Eshraghian, K.-R. Cho, O. Kavehei, S.-K. Kang, D. Abbott, and S.-M. S. Kang, "Memristor MOS content addressable memory (MCAM): Hybrid architecture for future high performance search engines," *IEEE Trans. Very Large Scale Integr. (VLSI) Syst.*, vol. 19, no. 8, pp. 1407–1417, Aug. 2011.
[8] S. Carrara, D. Sacchetto, M.-A. Doucey, C. Baj-Rossi, G. De Micheli, and Y. Leblebici, "Memristive-biosensors: A new detection method by using nanofabricated memristors," *Sens. Actuators B, Chem.*, vols. 171–172, pp. 449–457, Aug./Sep. 2012.
[9] I. Gupta, A. Serb, A. Khiat, R. Zeitler, S. Vassanelli, and T. Prodromakis, "Memristive integrative sensors for neuronal activity," 2015, *arXiv:1507.06832*.
[10] Y. V. Pershin and M. D. Ventra, "Experimental demonstration of associative memory with memristive neural networks," *Neural Netw.*, vol. 23, no. 7, pp. 881–886, 2010.
[11] J. Grollier, D. Querlioz, and M. D. Stiles, "Spintronic nanodevices for bioinspired computing," *Proc. IEEE*, vol. 104, no. 10, pp. 2024–2039, Oct. 2016.
[12] B. Sun *et al.*, "An organic nonvolatile resistive switching memory device fabricated with natural pectin from fruit peel," *Org. Electron.*, vol. 42, pp. 181–186, Mar. 2017.
[13] S. Battistoni, A. Dimonte, and V. Erokhin, "Organic memristor based elements for bio-inspired computing," in *Advances in Unconventional Computing*. Cham, Switzerland: Springer, 2017, pp. 469–496.
[14] D. B. Strukov, G. S. Snider, D. R. Stewart, and R. S. Williams, "The missing memristor found," *Nature*, vol. 453, no. 7191, pp. 80–83, 2008.
[15] C. Dias *et al.*, "Bipolar resistive switching in SI/AG nanostructures," *Appl. Surface Sci.*, vol. 424, pp. 122–126, Dec. 2017.
[16] S. Brivio, G. Tallarida, E. Cianci, and S. Spiga, "Formation and disruption of conductive filaments in a HfO2/TiN structure," *Nanotechnology*, vol. 25, no. 38, 2014, Art. no. 385705.
[17] B. Mohammad *et al.*, "State of the art of metal oxide memristor devices," *Nanotechnol. Rev.*, vol. 5, no. 3, pp. 311–329, 2016.
[18] S. Yu, H. Jiang, S. Huang, X. Peng, and A. Lu, "Compute-in-memory chips for deep learning: Recent trends and prospects," *IEEE Circuits Syst. Mag.*, vol. 21, no. 3, pp. 31–56, 3rd Quart., 2021.
[19] I. Messaris, A. Serb, A. Khiat, S. Nikolaidis, and T. Prodromakis, "A compact verilog—A ReRAM switching model," 2017, *arXiv:1703.01167*.
[20] P. S. Georgiou, S. N. Yaliraki, E. M. Drakakis, and M. Barahona, "Window functions and sigmoidal behaviour of memristive systems," *Int. J. Circuit Theory Appl.*, vol. 44, no. 9, pp. 1685–1696, 2016.
[21] A. Ascoli, R. Tetzlaff, and L. Chua, "Continuous and differentiable approximation of a TaO memristor model for robust numerical simulations," in *Emergent Complexity from Nonlinearity, in Physics, Engineering and the Life Sciences*. Cham, Switzerland: Springer, 2017, pp. 61–69.
[22] F. Jimenez-Molinos, M. Villena, J. Roldan, and A. Roldan, "A SPICE compact model for unipolar RRAM reset process analysis," *IEEE Trans. Electron Devices*, vol. 62, no. 3, pp. 955–962, Mar. 2015.
[23] Q. Li, A. Serb, T. Prodromakis, and H. Xu, "A memristor spice model accounting for synaptic activity dependence," *PloS One*, vol. 10, no. 3, 2015, Art. no. e0120506.
[24] J. Secco, F. Corinto, and A. Sebastian, "Flux-charge memristor model for phase change memory," *IEEE Trans. Circuits Syst. II, Exp. Briefs*, vol. 65, no. 1, pp. 111–114, Jan. 2018.
[25] R. Picos, J. B. Roldan, M. M. Al Chawa, P. Garcia-Fernandez, F. Jimenez-Molinos, and E. Garcia-Moreno, "Semiempirical modeling of reset transitions in unipolar resistive-switching based memristors," *Radio Eng.*, vol. 24, no. 2, pp. 420–424, 2015.
[26] R. Picos, J. B. Roldan, M. M. Al Chawa, F. Jimenez-Molinos, M. A. Villena, and E. Garcia-Moreno, "Exploring ReRAM-based memristors in the charge-flux domain, a modeling approach," in *Proc. Int. Conf. Memristive Syst.*, 2015, pp. 1–2.

[27] M. M. Al Chawa, R. Picos, J. B. Roldan, F. Jimenez-Molinos, M. A. Villena, and C. de Benito, "Exploring resistive switching-based memristors in the charge-flux domain: A modeling approach," *Int. J. Circuit Theory Appl.*, vol. 46, no. 1, pp. 29–38, 2018. [Online]. Available: http://dx.doi.org/10.1002/cta.2397
[28] M. M. Al Chawa, C. de Benito, and R. Picos, "A simple piecewise model of reset/set transitions in bipolar ReRAM memristive devices," *IEEE Trans. Circuits Syst. I, Reg. Papers*, vol. 65, no. 10, pp. 3469–3480, Oct. 2018.
[29] M. M. Al Chawa, R. Picos, and R. Tetzlaff, "A simple memristor model for neuromorphic ReRAM devices," in *Proc. IEEE Int. Symp. Circuits Syst. (ISCAS)*, 2020, p. 1.
[30] Z. Kolka, D. Biolek, V. Biolkova, and Z. Biolek, "Evaluation of memristor models for large crossbar structures," in *Proc. 26th Int. Conf. Radioelektronika*, 2016, pp. 91–94.
[31] R. Picos, J. Roldan, M. Al Chawa, F. Jimenez-Molinos, and E. Garcia-Moreno, "A physically based circuit model to account for variability in memristors with resistive switching operation," in *Proc. Conf. Design Circuits Integr. Syst. (DCIS)*, 2016, pp. 1–6.
[32] R. Naous, M. Al-Shedivat, and K. N. Salama, "Stochasticity modeling in memristors," *IEEE Trans. Nanotechnol.*, vol. 15, no. 1, pp. 15–28, Jan. 2016.
[33] M. M. Al Chawa, R. Tetzlaff, and R. Picos, "A simple Monte Carlo model for the cycle-to-cycle reset transition variation of ReRAM memristive devices," in *Proc. 9th Int. Conf. Modern Circuits Syst. Technol. (MOCAST)*, 2020, pp. 1–4.
[34] F. M. Puglisi, N. Zagni, L. Larcher, and P. Pavan, "Random telegraph noise in resistive random access memories: Compact modeling and advanced circuit design," *IEEE Trans. Electron Devices*, vol. 65, no. 7, pp. 2964–2972, Jul. 2018.
[35] S. Stathopoulos, A. Serb, A. Khiat, M. Ogorzałek, and T. Prodromakis, "Switching noise modelling in RRAM devices," in *Proc. Memrisys*, 2019.
[36] F. Corinto, P. P. Civalleri, and L. O. Chua, "A theoretical approach to memristor devices," vol. 5, no. 2, pp. 123–132, Jun. 2015.
[37] L. O. Chua, "Everything you wish to know about memristors but are afraid to ask," *Radio Eng.*, vol. 24, no. 2, p. 319–368, 2015.
[38] J.-M. Ginoux, B. Muthuswamy, R. Meucci, S. Euzzor, A. D. Garbo, and K. Ganesan, "A physical memristor based muthuswamy–Chua–Ginoux system," *Sci. Rep.*, vol. 10, no. 1, pp. 1–10, 2020.
[39] J. B. Roldán *et al.*, "On the thermal models for resistive random access memory circuit simulation," *Nanomaterials*, vol. 11, no. 5, p. 1261, 2021.
[40] J. S. Steinhart and S. R. Hart, "Calibration curves for thermistors," *Deep Sea Res. Oceanograph. Abstracts*, vol. 15, no. 4, pp. 497–503, 1968.
[41] A. Theodorakakos, S. G. Stavrinides, E. Hatzikraniotis, and R. Picos, "A non-ideal memristor device," in *Proc. Int. Conf. Memristive Syst. (MEMRISYS)*, 2015, pp. 1–2.
[42] D. Biolek, Z. Biolek, V. Biolková, and Z. Kolka, "Some fingerprints of ideal memristors," in *Proc. IEEE Int. Symp. Circuits Syst. (ISCAS)*, 2013, pp. 201–204.
[43] D. Maldonado *et al.*, "Experimental evaluation of the dynamic route map in the reset transition of memristive ReRAMs," *Chaos Solitons Fractals*, vol. 139, Oct. 2020, Art. no. 110288.
[44] F. Marrone *et al.*, "Phase-change memory as a memristive system: The state equations and dynamic route maps," submitted for publication.
[45] R. Picos, S. G. Stavrinides, A. Theodorakakos, and E. Hatzikraniotis, "The experimental model of a non-ideal memristor," in *Proc. 5th Int. Conf. Modern Circuits Syst. Technol. (MOCAST)*, 2016, pp. 1–4.
[46] D. Clauss, R. Ralich, and R. Ramsier, "Hysteresis in a light bulb: Connecting electricity and thermodynamics with simple experiments and simulations," *Eur. J. Phys.*, vol. 22, no. 4, p. 385, 2001.
[47] Z. Biolek, D. Biolek, J. Vavra, V. Biolkova, and Z. Kolka, "The simplest memristor in the world," in *Proc. IEEE Int. Symp. Circuits Syst. (ISCAS)*, 2016, pp. 1854–1857.
[48] F. Corinto and M. Forti, "Memristor circuits: Flux—Charge analysis method," *IEEE Trans. Circuits Syst. I, Reg. Papers*, vol. 63, no. 11, pp. 1997–2009, Nov. 2016.
[49] D. R. Lide, *CRC Handbook of Chemistry and Physics*. Boca Raton, FL, USA: CRC Press, 2012.
[50] C. H. Shomate, "A method for evaluating and correlating thermodynamic data," *J. Phys. Chem.*, vol. 58, no. 4, pp. 368–372, 1954.

RODRIGO PICOS (Senior Member, IEEE) received the M.S. and Ph.D. degrees from the Universitat de les Illes Balears, Palma (Illes Balears), Spain, in 1998 and 2006, respectively.

He is currently a Professor with the Industrial Engineering and Construction Department, University of Balearic Islands and a Member of the Balearic Islands Health Institute (IdISBa) Palma, Mallorca, Spain. He has taught courses on Electron Device Modeling, Electronic Instrumentation, and basic Electronics. He has authored or coauthored more than 120 journal and conference papers. He has participated as a Researcher in several national and international (EU) funded projects. His research interests include memristive systems and compact-device modeling, as well as analog circuit design and test.

MOHAMAD MONER AL CHAWA (Member, IEEE) received the M.S. degree in advanced communication engineering from Damascus University, Damascus, Syria, in 2013, and the Ph.D. degree in electronic engineering from the Universitat de les Illes Balears, Palma, Spain, in 2019. He is currently a Research Associate with the Institute of Circuits and Systems, Technische Universität Dresden. His research interests include memristive systems, device modeling, and circuit design.

CAROLA DE BENITO (Senior Member, IEEE) received the M.S. degree in physics and the Ph.D. degree in electronic engineering from the Universitat de les Illes Balears (UIB) in 1991 and 2012, respectively.

She is currently an Associate Professor with the Electronic Technology Group, Industrial and Construction Engineering Department, UIB. She has authored or coauthored more than 25 journal and conference papers and she has participated in several national and international projects. Her research interests include device and circuit modeling low-temperature CMOS design and memristor device and memristive system modeling.

STAVROS G. STAVRINIDES (Senior Member, IEEE) received the M.Sc. degree in electronics and the Ph.D. degree in chaotic electronics from the Aristotle University of Thessaloniki, Greece, where he is a Physicist. He has taught numerous topics in physics and electronics in academia, as an Adjunct Lecturer, for more than 12 years, while from 2012 to 2013 he was with the ECE Department, University of Cyprus, as a Visiting Assistant Professor. He currently serves as a Faculty Member with the School of Science and Technology, International Hellenic University, Thessaloniki, Greece. He has authored or coauthored more than 90 journal and conference papers. He has participated as a Researcher in several national and international (EU, NATO) funded projects. His research interests include, non-exhaustively, chaotic electronics and their applications (with emphasis on security), econophysics, nonlinear time series analysis, memristors, and experimental chaotic synchronization.

LEON O. CHUA (Life Fellow, IEEE) was a Foreign Member of the European Academy of Sciences (Academia Europaea) in 1997 and the Hungarian Academy of Sciences in 2007. He is widely known for his invention of the Memristor. When not immersed in Science, he relaxes by searching for Wagner's leitmotifs, musing over Kandinsky's chaos, and contemplating Wittgenstein's inner thoughts. His research has been recognized through 17 honorary doctorates from major universities in Europe and Japan, and holds seven U.S. patents. He has been conferred numerous prestigious awards, including the first Kirchhoff Award, the Guggenheim Fellow, the 2019 EDS Celebrated Member Prize—The Highest Recognition of the IEEE Electron Devices Society, and the 2020 Julius Springer Prize in Applied Physics. He was elected as a member of the Confrerie des Chevaliers du Tastevin in 2000.